Naval Research Laboratory

Washington, DC 20375-5320

NRL/MR/6707--00-8463

Plasma Acceleration by Area Expansion

WALLACE M. MANHEIMER

Senior Scientist, Fundamental Plasma Processes

RICHARD FERNSLER

Charged Particles Physics Branch
Plasma Physics Division

June 26, 2000

20000710 064

DTIC QUALITY INSPECTED 4

REPORT DOCUMENTATION PAGE

Public reporting burden for this collection of information is estimated to average 1 hour per response, including the time for reviewing instructions, searching existing data sources, gathering and maintaining the data needed, and completing and reviewing the collection of information. Send comments regarding this burden estimate or any other aspect of this collection of information, including suggestions for reducing this burden, to Washington Headquarters Services, Directorate for Information Operations and Reports, 1215 Jefferson Davis Highway, Suite 1204, Arlington, VA 22202-4302, and to the Office of Management and Budget, Paperwork Reduction Project (0704-0188), Washington, DC 20503.

1. AGENCY USE ONLY (*Leave Blank*)	2. REPORT DATE June 26, 2000	3. REPORT TYPE AND DATES COVERED Interim	
4. TITLE AND SUBTITLE Plasma Acceleration by Area Expansion			5. FUNDING NUMBERS
6. AUTHOR(S) Wallace M. Manheimer and Richard Fernsler			
7. PERFORMING ORGANIZATION NAME(S) AND ADDRESS(ES) Naval Research Laboratory Washington, DC 20375-5320			8. PERFORMING ORGANIZATION REPORT NUMBER NRL/MR/6707--00-8463
9. SPONSORING/MONITORING AGENCY NAME(S) AND ADDRESS(ES) Office of Naval Research 800 N. Quincy Street Arlington, VA 22217			10. SPONSORING/MONITORING AGENCY REPORT NUMBER
11. SUPPLEMENTARY NOTES			
12a. DISTRIBUTION/AVAILABILITY STATEMENT Approved for public release; distribution is unlimited.			12b. DISTRIBUTION CODE

13. ABSTRACT (*Maximum 200 words*)

As the area of a plasma increases, the plasma can accelerate smoothly from subsonic to supersonic velocity. The singularity which ordinarily occurs at the sonic velocity is resolved not by charge separation, as is the case for a sheath; but rather by a zero in the numerator at the same spatial position as the zero in the denominator, the sonic point. That is, at the sonic point, the acceleration due to expansion just cancels out the deceleration due to ion and electron neutral collisions. It turns out that in this configuration, the plasma can accelerate to about three times the ion sound speed. The electron temperature is determined by the geometry, gas species, and mostly, by the gas pressure. Applications to the production of a stream of neutrals for etching, and to space plasma propulsion are discussed.

14. SUBJECT TERMS			15. NUMBER OF PAGES 31
			16. PRICE CODE
17. SECURITY CLASSIFICATION OF REPORT UNCLASSIFIED	18. SECURITY CLASSIFICATION OF THIS PAGE UNCLASSIFIED	19. SECURITY CLASSIFICATION OF ABSTRACT UNCLASSIFIED	20. LIMITATION OF ABSTRACT UL

1. Introduction

Plasmas are almost always at some positive voltage compared to their bounding surfaces. However most of this voltage drop occurs in a sheath region near the walls. For instance if the plasma has an electron temperature T_e and draws no dc current (the usual condition for processing plasmas in an insulating chamber), the sheath potential ϕ_{sh} is the floating potential [1]

$$e\phi_{sh} = \frac{T_e}{2} \ln\left(\frac{M}{2\pi m}\right) \qquad (1)$$

where m and M are the electron and ion masses. An ion accelerating through this sheath strikes a substrate with this energy. By contrast, the Bohm condition [2] appears to specify that the ion can only accelerate to an energy of $T_e/2$ in the plasma bulk. Thus for say an argon plasma, nearly ten times the voltage drop is across the sheath.

However, for certain applications, we would like to accelerate ions to this sort of energy while they are in the plasma bulk. The two applications which we have in mind are plasma processing with a stream of neutrals [3,4], and space propulsion (i.e. a plasma thruster) [5]. In the former, the idea is to reduce charge damage to the substrate being processed. One possibility is to convert the stream of ions, with energy of some tens of volts, into a stream of neutrals. This would be done by taking the ion stream and passing it through a neutralizing gas cell and exploiting the fact that the mean free path for charge exchange is considerably less than that for neutral-neutral collisions. Since the ion neutral charge exchange mean free path length is orders of magnitude greater than the sheath thickness, this can only be done if the ions are somehow accelerated in the bulk plasma. For the thruster, the accelerated ions, and their neutralizing electrons, are ejected into space, and not into a wall.

The Bohm condition for a plasma sheath interface is well known, and it says that at the sheath edge, the plasma velocity is the ion sound speed. At this velocity, the steady state quasi-neutral fluid equations for the plasma become singular and this singularity is resolved by accounting for charge separation in the sheath. The question then becomes how can the quasi-neutral plasma accelerate to supersonic velocity? The answer is that there are other ways in which this singularity can be resolved. In the fluid equations for the steady state plasma, the singularity occurs when the denominator in the equation for say du/dx vanishes. This singularity can also be resolved if the numerator also vanishes; that is, the acceleration due to area expansion just cancels the deceleration due to neutral collisions.

In order for the electron and ion currents to equalize at the wall, an ion rich sheath must still form. However a sheath can always form in a supersonic plasma, so no

additional condition is necessary. Recall that in the derivation of the Bohm condition [2], for a sheath to form, the ion velocity has to be supersonic. Thus to form a sheath, a subsonic plasma has to accelerate to the sound speed at the sheath edge. But if the plasma enters the sheath at a faster speed, no additional condition is required to form the sheath.

The simplest example is a gas nozzle, where because of area change, a neutral fluid can make a smooth transition from subsonic to supersonic flow [6]. Other examples occur throughout plasma physics [7,8]. Riemann, in his work on the Bohm condition has also recognized that the standard Bohm condition can be modified if the plasma area expands [9]. We discuss here the analogous example of a quasi-neutral plasma nozzle. We find that with area expansion, one can accelerate the plasma to a maximum of about three times the sound speed. Furthermore, one achieves this acceleration without either additional power supplies (the power which forms the plasma also powers the acceleration) or fine screens in the plasma. The latter especially can be a serious constraint on either plasma processing systems, which often work with corrosive gases, or on plasma thrusters, which have a requirement for long life.

While the theory presented here can be applied to any plasma which has an area which increases along the axis of acceleration, we think here mostly of plasmas produced by electron cyclotron resonance (ECR). An ECR plasma is formed by absorbing microwave radiation (usually at 2.45 GHz) at the position of cyclotron resonance (where B=875G). There are basically two possible configurations for an ECR plasma. In the first, the magnetic field is axial and the microwave power is injected into a decreasing magnetic field. In this configuration the plasma density can be much greater than the critical density. The right hand circularly polarized wave can propagate in from the outside, and it is absorbed at the position of cyclotron resonance. The magnetic field is generally produced by coils and the field has a spatial profile which decreases along the axis of acceleration. The outermost field line defines the plasma edge [10,11].

In the second configuration, the field is produced by a series of cusps. The plasma is confined by the surface fields, and there is no field in the center. The microwave power is injected radially, usually through a coaxial coupler. The area increases simply by moving the magnets further and further away from the axis. The position of cyclotron resonance is not as simple, but if the magnets are strong enough there will be positions of cyclotron resonance along the edge. Experience has confirmed that high density plasmas can be formed this way as well [12]. In either case, the plasma strongly absorbs the microwave radiation at the position of ECR. Schematics of each configuration are shown in Fig 1 a and b.

In Section 2, we describe the basic steady state theory of the quasi-neutral ECR plasma nozzle and give various estimates and an upper limit for the acceleration. Section 2 describes the acceleration relative to the sound speed by the area increase. Other

aspects of the problem include the calculation of plasma density and temperature as well as neutral density (for the case of a strongly ionized plasma). Qualitative estimates for these quantities are given in Section 3 by the application of conservation laws. While this is not a complete solution to the problem, it does give a simple and physical description of two important regimes, high and low pressure. In the high pressure regime, the electron temperature is determined by ionization balance, and the plasma density by energy balance. In the low pressure regime, the ion density is determined by mass flow, the temperature by power balance, and the neutral density by ionization balance. For a typical laboratory argon plasma, the transition pressure is roughly 10^{-4}torr. This model is then applied to a recent series of experiments on ECR plasmas [13-16].

Section 4 describes the application to neutral etching. In the quasi-neutral plasma nozzle, the ions are accelerated to the required energy and then pass through a neutral gas, charge exchange, and become a neutral stream. Section 5 briefly discusses the possibility of the quasi-neutral ECR plasma nozzle as a space thruster. Indeed, recent theoretical work on the Hall thruster has exploited the same transition from subsonic to supersonic flow investigated here [17-18]. Potential advantages of the ECR nozzle include high thrust, high specific thrust, and high efficiency. Also the scheme does not employ grids or high voltage and it has the additional advantage of operating with low plume divergence angle.

2. A Quasi-neutral ECR Plasma Nozzle

Let us consider quasi-neutral a plasma with an area $A(x)$ which varies with x. For the case of an ECR plasma with an axial magnetic field magnetic field $B(x)$, the area $A(x)$ of the plasma will be determined by $B(x)A(x) = $ constant. In steady state, the plasma continuity equation reduces to the one dimensional equation

$$\frac{d}{dx} nuA = SA \tag{2}$$

where n is the number density, u is the flow velocity, and S is the ionization source. We assume the ionization is caused by electron impact ionization and neglect recombination. Thus

$$S = \beta(T_e)nN \equiv \omega(T_e)n \tag{3}$$

where N is the background neutral density, and β is the average of the ionization cross section times the electron velocity. The force equation comes from taking the total momentum equation (electron plus ion, but neglecting electron inertia) and subtracting u times the density equation. When doing this, there turn out to be two collisional terms which decelerate the ions. The first is the ion momentum exchange collisions with frequency ν_i. These collisions are mainly charge exchange collisions. The second term is the effect of ionization. When an ion is produced, it is assumed to be produced at zero velocity. If the ions are flowing and an additional ion is produced at rest by impact ionization, the ion fluid slows down. The force equation for the plasma in steady state then turns out to be

$$Mu\frac{du}{dx} = -\frac{T_e}{n}\frac{dn}{dx} - M(\nu_i + \omega)u \tag{4}$$

Here we have assumed that $M\nu_i \gg m\nu_e$, where ν_e is the electron-neutral collision frequency. Even though the electron mean free path is not short compared to the length of the system, the electrons are still isotropic because they are electrostatically confined in z. That is, they bounce back and forth many times before leaving the system, and their mean free path is short compared to the total distance they travel before leaving the system. Therefore their pressure is isotropic. Because of the long mean free path length of the electrons, they are approximately isothermal.

Equations (2 and 4) can be combined to yield two separate equations for $n' \equiv dn/dx$, and $u' \equiv du/dx$. These are

$$\frac{du}{dx} = \frac{Mu^2(v_i + \omega) + T_e\left(\omega - u\frac{d}{dx}\ln A\right)}{T_e - Mu^2} \qquad (5)$$

and

$$\frac{d}{dx}\ln n = -\frac{1}{u}\left[\frac{Mu^2\left(v_i + 2\omega - u\frac{d}{dx}\ln A\right)}{T_e - Mu^2}\right] \qquad (6)$$

There two comments to make. First, the equation for n is only an equation for the relative density, and it involves only u, not n, on the right hand side. Second, the equations appear to be singular where the flow velocity is equal to the sound speed c_s ($=[T_e/M]^{1/2}$). However because of the variation of area with x, this is no longer necessarily the case. Specifically the numerator can also vanish when the denominator vanishes. That is the singularity vanishes when

$$c_s\frac{d}{dx}\ln A = v_i + 2\omega \qquad (7)$$

at the sonic point ($u=c_s$).

Consider now the approximate sizes of v_i and ω for oxygen (for the neutral etcher) and helium or argon (for the thruster). A reasonable approximation for v_i in all three gases [19-22] at ion energies of interest (1ev<E<200ev) is

$$v_i(s^{-1}) \approx 10^{-9}E^{0.2}(ev)N(cm^{-3}) \qquad (8)$$

where E is the ion energy.

The ionization rate is given by $N\langle\sigma_i v_e\rangle$ where σ_i is the ionization cross section and v_e is the electron velocity. To estimate $\langle\sigma_i v_e\rangle$, we use data from Brown [23] and assume that σ_i is zero below the ionization energy ε_i, increases linearly with energy to a value of σ_o at an energy of $4\varepsilon_i$, and then remains constant. For the electron distribution function we take a Maxwellian at temperature T_e. Note that in discussing plasmas at high density ($n \sim 10^{12}$ cm^{-3}) and low temperature ($T_e\sim5eV$), electron-electron collisions strongly drive the electron distribution function to a Maxwellian. Quasi-neutral particle simulations of such high density plasmas indeed show that electron distributions tend to

be Maxwellian [10]. This and the NRL ECR etcher experiment [11] also show that the electron temperature is reasonably constant along a field line.

Making these assumptions, we find that the ionization rate is given by

$$\omega = N\sigma_o \sqrt{\frac{2T_e}{\pi m}} F\left(\frac{T_e}{\varepsilon_i}\right) \tag{9a}$$

where

$$F\left(\frac{T_e}{\varepsilon_i}\right) = \left(\frac{1}{3} + \frac{2T_e}{3\varepsilon_i}\right) \exp\left(-\frac{\varepsilon_i}{T_e}\right) - \left(\frac{4}{3} + \frac{2T_e}{3\varepsilon_i}\right) \exp\left(-4\frac{\varepsilon_i}{T_e}\right) \tag{9b}$$

A plot of $F(T_e/\varepsilon_i)$ as a function of T_e/ε_i is shown in Fig. (2). For low temperature, $F(T_e/\varepsilon_i)$ approaches $(1/3)\exp(-\varepsilon_i/T_e)$, and for large temperature it approaches unity. For an oxygen plasma, with $\sigma_o \approx 2\times10^{-16} cm^2$ and $T_e \approx 4eV$, v_i is about equal to ω. For an argon or helium plasma, σ_o is about the same. However the ionization energy for helium is 25 ev, rather than the more typical 12-15 ev for most other gases.

For a gas density $N = 3\times10^{13} cm^{-3}$ (1 mtorr), $T_e = 4eV$, and v_i and ω given by Eqs. (8 and 9) we find that the expansion scale length for A(x) at the sonic point is about 10 cm. Thus we envision a plasma with an area as a function of x which looks as shown in Fig (1). There, x_s is the sonic point, and x_w is the left hand wall, say the position of the vacuum window on the microwave system. To the left of x_s the plasma is subsonic, and to the right it is supersonic. At some position x_r to the right of the sonic point, x_r, the area flattens out (the magnetic field becomes uniform) and a supersonic plasma flows into the uniform region. For the neutral etcher, charge exchange forms the neutral beam. For the thuster, the plasma flux simply exits into space.

Near the sonic point, assume that

$$u(x) = \frac{du}{dx}(x - x_s) \tag{10}$$

Inserting this expression on the right hand side of Eq. (5), we find that du/dx satisfies a quadratic equation

$$\left(\frac{du}{dx}\right)^2 - \left[\frac{c_s}{2}\left(\frac{d}{dx}\ln A\right) - v_i - \omega\right]\frac{du}{dx} - \frac{c_s^2}{2}\frac{d^2}{dx^2}\ln A = 0 \tag{11}$$

6

If the last term is positive, there is one positive root and one negative root for u' at the sonic point. Clearly the positive root is taken for plasma acceleration. Thus we can now initialize u', and thereby n', and integrate Eqs. (5 and 6) in either direction from the sonic point.

Let us first consider the integration toward x_w. The derivative of u is positive, and remains positive until u' becomes singular a second time at negative velocity. According to the standard Bohm condition, this singularity occurs at the wall x_w. However the singularity can occur at x_w only if there is a free parameter in the equations. For the standard case of a high pressure discharge (P> 10^{-3} torr), this free parameter is the electron temperature, and the parameter which depends most strongly on T_e is ω. T_e and ω thus self adjust until the Bohm condition is satisfied at the wall. This is the familiar way of determining the velocity and relative density profile of a discharge. In the next section we will discuss discharges at low pressure.

Integrating Eq. (5) towards positive x gives the acceleration of the plasma. This acceleration is determined by the dependence of area on x. Notice that once the geometry is specified, the exiting velocity is also specified. Thus in designing a system, one decides on the exit velocity and designs for it.

We now discuss an approximate solution for the final velocity u_r on the right hand edge. Equation (5) contains terms which accelerate the supersonic plasma due to area expansion, and other terms which describe the various collisional slowing down processes. If we consider the neutrals as flowing from the low area source and out at the high area, this neutral flow pattern will naturally reduce the neutral density in the acceleration region. If we neglect the collisional slowing down, Eq. (5) can be integrated for the velocity as a function of area. This then gives an approximate upper limit for energy as a function of area. If one can control the neutral density as a function of x, it would be advantageous to minimize it in the acceleration region somewhat beyond the sonic point, so that the calculated upper limit would not be too bad an approximation. Integrating Eq. (5) with the collision terms neglected, we find that the upper limit for ion energy E as a function of area A is

$$\frac{E}{T_e} - \frac{1}{2}\left(1 + \ln\frac{2E}{T_e}\right) = \ln\frac{A}{A_o} \qquad (12)$$

where A_o is the area at the sonic point where $E/T_e = \frac{1}{2}$. A plot of the upper limit of energy as a function of area is shown in Fig (3). For an area increase of about a factor of 25, or a radius increase of about a factor of 5, the energy increases by nearly a factor of 10, to about 5 times T_e. For larger area increases, the energy increases much more slowly. Thus in practice, an increase in ion energy by about an order of magnitude is a

reasonable estimate of the maximum possible ion acceleration. At the position of the right hand boundary, $x=x_r$, let us define $u = \alpha c_s$, where α is the amount of acceleration in the expanding region; it depends on the design of the system. As we have seen, α may be as large as perhaps 3.

Without the collisions, the density equation is also simple to integrate, and thus upper limit from Eq. (2) is

$$nuA = n_s c_s A_o \qquad\qquad\qquad (13)$$

where n_s is the density at the sonic point. A plot of energy as a function of density is shown in Fig. 4. Thus if the area increases a factor of 25 from the sonic point, and the velocity by a factor of three, the density decreases by about a factor of 75 from the sonic point. If we assume a high density plasma, with $n_s \sim 2 \times 10^{12}$, cm^{-3}, the density of plasma exiting will be about 3×10^{10} cm^{-3}.

3. Conservation Laws

In this section we give approximate calculations of the plasma temperature, the plasma and neutral density, and the flow. Instead of a fluid equation for the neutrals, conservation laws are used. Conservation laws are particularly useful in high pressure, weakly ionized gases where the neutral flux is largely unperturbed; and also in low pressure, strongly ionized gases where the mass flux out is dominated by the ion flux. In a future work we will examine more fully the role of the neutral flow.

The first conservation law is ionization balance. Integrating Eq. (2) over the length of the ionization region, we find

$$\sum_a n_a A_a \sqrt{\frac{T_e}{M}} = N\sigma_o L \sqrt{\frac{2T_e}{\pi m}} \overline{nA} F(T_e / \varepsilon_i) \tag{14}$$

where $L = x_s - x_w$ is the length of the system between the two sonic points, a is an index which denotes the position at the sonic points (w for the left sonic point, s for the right sonic point), and we have assumed no ionization in the acceleration region $x > x_s$. Here $\overline{nA}$ is the average value of ion density times area between the two sonic points. Usually we will assume there is not much variation in area between the two sonic points.

Equation (14) is an equation for T_e/ε_i and is plotted in Fig. (5). At high pressure, the temperature is low and is a slowly varying function of pressure. In this regime, $T_e \sim \varepsilon_i/3$ However as N decreases, T_e rises, ultimately sharply. In fact when $T_e > \varepsilon_i$, $F(T_e/\varepsilon_i)$ approaches unity and Eq. (14) becomes an equation for the neutral density N. For an argon plasma with $\sigma_o = 2x10^{-16}$ cm^2, L = 40 cm, and $\overline{n}/n_s = 5$, [10] this neutral density is about $2.3x10^{11}$cm^{-3}. This is the minimum neutral density that can support the discharge. The actual neutral density, before the discharge is struck, must of course be higher because some of the neutrals are ionized. Both Ono's ECR experiment [14], and initial results for the NRL ECR neutral etcher experiment [24] show that one cannot strike a discharge at densities below this value.

We now consider the energy balance. To do so, we consider the energy flux out both ends of the system and equate it to the power deposited in the system by the microwaves. Again we assume that there is no ionization in the acceleration region, so that nuA is constant there. This allows us to once again compare the energy flux out the end with the energy flux through the sonic point.

Each ion and electron carries out of the plasma the energy E_i needed to produce an electron ion pair, as well as the kinetic energy (only the ions have significant kinetic energy) and the thermal energy (only the electrons are assumed to have thermal energy).

The quantity E_i is not the ionization energy because there are other channels for energy loss than ionization, for instance radiation and the production of metastables. The energy balance equation is then

$$\sum_a A_a n_a \sqrt{\frac{T_e}{M}} \left[\frac{1}{2} \alpha_a^2 T_e + \frac{5}{2} T_e + E_i \right]_a = P_\mu \tag{15}$$

Recall that α_s is the amount of acceleration in the region of area expansion, about three or less, and that $\alpha_w = 1$. For both the thruster and neutral etcher, it is advantageous to design the system so as to keep the wall density n_w as small as possible.

The remaining conservation law is the conservation of total mass, ion plus neutral. Before the discharge is struck, there is a gas input I_0 in particles per second, and a gas pumping speed, PU, in volume per second. This gives rise to a neutral density, $N_0 = I_0/PU$. If these neutrals are vented out through x_s, the neutral velocity out is $v_N = PU/A_s$.

When the discharge is struck, the plasma changes the flow dynamics to

$$n_s \sqrt{\frac{T_e}{M}} + N v_N = I_0 \tag{16}$$

Notice that we do not consider the loss of mass at x_w. The reason is that neutrals bounce off and do not stick, whereas ions recombine at the wall and rejoin the neutral stream. Thus while Eq. (15) shows that the left wall is a sink for energy, Eq. (16) shows that it is not a sink for particles.

Equations (14-16) are the three conservation laws which determine the plasma electron temperature, plasma density, and neutral density in terms of the system design parameters, I_0, P_μ, gas type, geometry, etc. There are two simple limits in which analytic solutions are possible, and we summarize them here. They are high pressure (typically above a 1 mtorr), where

$$F \approx \frac{1}{3} \exp\left(-\frac{\varepsilon_i}{T_e} \right) \tag{17}$$

and low pressure (typically below about 100 μtorr) , where

$$F \approx 1 \tag{18}$$

In the former regime, the plasma is weakly ionized and $Nv_N >> nc_s$. In that case the neutral density is unaffected by the plasma. The electron temperature is then given from Eq. (14) by

$$T_e = \frac{\varepsilon_i}{\ln\left\{\sqrt{\frac{2M}{\pi m}}\,\frac{N\sigma_o L}{6\left(\frac{n_s}{n}\right)}\right\}} \tag{19}$$

while the electron density at the sonic point is given from Eq. (15) by

$$n_s = \frac{P_\mu}{A_s\sqrt{\frac{T_e}{M}}\left[\frac{1}{2}\left(\alpha_s^2+1\right)T_e + 5T_e + 2E_i\right]} \tag{20}$$

where for convenience we have assumed the densities and areas are the same at the two sonic points. In the high pressure regime, we obtain the usual result that the electron temperature is governed by the ionization balance, while the plasma density is governed by the power balance. The pumping rate and neutral dynamics decouple from the plasma generation, and the plasma is weakly ionized.

A strikingly different result is obtained in the low pressure regime where F is given by Eq. (18). We assume that the mass flux is dominated by the supersonic plasma exhaust. For either the etcher or thruster, the goal is to design the system so as to minimize flux of energy into x_w. The energy balance gives the electron temperature as

$$T_e = \frac{\dfrac{P_\mu}{2I_o} - E_i}{\left(\dfrac{\alpha_s^2}{2} + \dfrac{5}{2}\right)} \tag{21}$$

where again we assumed that n and A are the same at the two sonic points. Curiously, at low pressure, Eq. (14) for the ionization balance determines the neutral density,

$$N = 2\sqrt{\frac{\pi m}{2M}}\,\frac{n_s A_s}{nA}\,\frac{1}{L\sigma_o} \tag{22}$$

while Eq. (15) for mass flux determines the plasma density

$$n = \frac{I_o}{A_s\sqrt{\dfrac{T_e}{M}}} \tag{23}$$

since the plasma is now strongly ionized and the ion velocity is assumed to be considerably greater than the neutral velocity. That is, now the plasma density is specified by the mass input, and the temperature is specified by the power input. In between these limits, the electron temperature as a function of pressure can be determined from Fig. (4).

The one quantity not yet determined is E_i, the energy to create an electron ion pair. This is the ionization energy plus the energy lost through all other loss channels. These other channels are inelastic collisions due to the various excitations of the atom or molecule. For a steady state plasma with an electron distribution function $f(v)$, the power lost by the electrons due to ionization and all excitations is

$$P_{ion} = N\int d^3v \left(\sigma_i\varepsilon_i + \sum_{ex}\sigma_{ex}\varepsilon_{ex} \right) vf(v) \tag{24}$$

where ε_i is the ionization energy, ε_{ex} is the excitation energy and the summation is over all excitations. The rate of ion production is given by

$$\omega = N\int d^3v\sigma_i vf(v) \tag{25}$$

Therefore, the energy expended to produce an electron ion pair, counting all of the associated excitation is simply

$$E_i = \frac{P_{ion}}{\omega} \tag{26}$$

For the high pressure ECR plasma, a microwave field at the cyclotron resonance is like a dc field in a discharge. Thus a great deal of insight can be obtained from the swarm relations for a discharge. The first Townsend coefficient, α_T, is the number of ions an electron produces per centimeter of its drift. The energy gained per cm of drift equals eE_f where E_f is the electric field. Thus

$$E_i \text{ (eV)} = eE_f(eV/cm)/\alpha_T(cm^{-1}) \equiv \frac{E_f/N}{\alpha_T/N} \tag{27}$$

12

Dutton [25] tabulates α_T/N as a function of E_f/N. The experiments and the calculations that constitute Dutton's tabulations are for low electron density, so that electron electron collisions are insignificant compared to electron neutral collisions. In all cases, ionization must compete with excitations and metastable generation, which have lower thresholds than ionization. These lower energy excitations deplete the tail of the electron distribution function; the tail is repopulated by the accelerating electric field. However at high electron density, electron electron collisions further repopulate the tail, so that ionization is greater than predicted from swarm data. Therefore, swarm data overestimates E_i.

The next question is what are α_T/N and E_f/N in the ECR plasma. The condition for creating the plasma is that the ionization rate has to be equal to the loss rate. The ionization rate is simply the drift velocity, u_d in the electric field times α_T (i.e. $\omega = u_d\alpha_T$). The loss rate for the ECR plasma is roughly the sound speed divided by the half length of the plasma L, or

$$u_d\alpha_T / N = c_s / NL \qquad (28)$$

Dutton also tabulates data for u_d as a function of E_f/N. Assuming $T_e = 4$ ev for argon, oxygen and xenon, we find values of E_i of 57 ev for argon, 70 ev for oxygen, and 38 ev for xenon. These values are of course approximate and depend on NL, but show they that for rare gases, $E_i \sim 3\varepsilon_i$, while for diatomic gases, $E_i \sim 6\varepsilon_i$. A similar calculation shows $E_i = 65$ eV for helium at 7 ev, where we have assumed the higher temperature because of the higher ionization energy.

We now consider the different situation of ionization by an energetic electron beam. In this case, the energy to produce an electron ion pair plus the energy of the recoil electrons E_e has been tabulated for a variety of gases and at a variety of beam energies [26]. There is strikingly little variation in E_i. Typically this energy is between 30 and 40 eV for most monatomic and diatomic gases having ε_i of around 15 eV. Also E_e is typically a few ev, so it is small compared to E_i. Ionization by the beam is therefore relatively efficient with perhaps one third to one half of the energy lost going into ionization. An electron beam is probably the most efficient way to generate a plasma. The swarm data overestimates the energy going into other loss channels, the beam model underestimates it. However the estimates are only different by a factor of two for rare gases. Thus an ECR discharge at pressure ranges of milli-torr and below is a rather efficient way of producing plasma.

We now discuss these results in the light of a recent series of experiments on argon ECR plasmas [13-16]. In these experiments, an ECR plasma, in the axial configuration of Fig. (1a) was generated by microwave power at 2.4 GHz. The magnetic field decreased from about 1 kG to much lower values over about 40 cm. The actual

lower value depended on the current in a downstream trim coil, and the magnetic field configuration could be varied from mirror, to conventional ECR configuration, to cusp. We consider here the results for ECR configuration, where the downstream field is about 40 G, so that according to Fig. (3), the maximum ion energy at the probe would be between about 4 and 5 times the electron temperature.

Typically a beam like distribution of ions was observed downstream [13]. The ion energy within the plasma, at 40 cm from the microwave window (where $B \approx 40$ G) is measured with an ion energy analyzer as a function of a number of parameters including gas pressure. The measured ion energy as a function of pressure is shown in Fig. (7). (The data in Ref. (13) are reported in Pascals, where 1 Pa = 7.6×10^{-3} torr.) Also shown in the figure is the calculated ion energy. The calculation was done in the following way.

The electron temperature as a function of pressure is obtained from Fig. (5). At the lowest pressure, the ratio of measured ion energy to calculated electron temperature is 4.3. The graph in Fig. (6) is a plot of 4.3 times the calculated electron temperature as a function of pressure. As is apparent, the fit is reasonably good. The experiment was done in the regime in which neither Eq. (17 nor 18) is very accurate. However the pressure regime is still high in the sense that Eq. (14) was used to calculate the electron temperature rather than neutral density. The measured curve in Fig. (6) falls off with pressure somewhat faster than the calculated curve. However this could be because at the higher pressure, the ion flow is more collisional. Using Eq. (7) for the collision frequency for argon, we see that at the highest pressure, the mean free path of a 20 eV argon ion is about 25 cm.

To summarize, in the last section we calculated the acceleration from a plasma with an expanding area. In this section we used conservation laws to estimate the plasma density and temperature. We compared the model with a recent series of experiments on an ECR plasma and found generally good agreement.

A better model would be to use quasi-neutral particle [10] simulation. As discussed here, the boundary condition in the simulation needs to be a modified Bohm condition, which specifies that the *minimum* ion velocity at the wall is the ion sound speed. This is because a quasi-neutral plasma can only make a transition into the wall sheath if the ion fluid velocity is equal to or *greater* than the sound speed. In a future work, we will give designs of an ECR plasma neutral etcher based on numerical simulations.

4. The Neutral Etcher:

The quasi-neutral ECR plasma nozzle could make an attractive neutral etcher. We assume a configuration like Fig 1a (or possibly Fig 1b). Just to the right of the wall, $x=x_w$, there is a plasma sheath which raises the plasma potential to a value approximately given by Eq. (1). To the right of x_w the plasma starts as a conventional ECR plasma. Then in the expanding region, the plasma is accelerated to a kinetic energy of perhaps as much as five to ten times its value at the sonic point. In this acceleration region, the goal is to reduce as much as possible the neutral density, (while keeping a relatively larger value in the plasma production region). After x_r, the plasma area remains constant. This is the charge exchange region, of length roughly twice the charge exchange mean free path, (which is much shorter than the neutral neutral mean free path) where the stream of fast ions becomes a stream of neutrals. The length of this charge exchange region would be optimized (as a function of gas pressure) so as to produce the maximum flux of neutrals on the workpiece being processed. Notice that as the flowing plasma charge exchanges, it leaves in its wake not only a flux of fast neutrals, but also a plasma with low velocity. Moreover the ion and fast neutral fluxes are nearly equal.

If this low velocity plasma is allowed to contact the workpiece, it will form an additional sheath that would accelerate the ions into the workpiece. The potential of the surface to the far right would be determined by the total potential change across the plasma, including the potential drop in each sheath. (Recall that we assume the boundary condition is zero current density on the bounding surface to the right and to the left; the potentials float to whatever is necessary to impose this zero current condition.) The ion energy falling through this sheath on the right is about the same as the neutral energy. If the ions are not a problem for the particular process, they could be allowed to impinge on the workpiece. Otherwise the plasma should be deflected. For the case of an axial field, the simplest way to do this is to symmetrically deflect the magnetic field lines into a side wall, and right before the workpiece, deflect the remnant field, most likely with a small permanent magnet. This is illustrated in Fig 7. There the neutrals would go straight to the workpiece, while the plasma would deflect to the side walls and the sheath would form there. If the neutral density is 3×10^{10} cm^{-3}, which seems achievable if the density at the sonic point is a few times 10^{12} cm^{-3}, and the gas is molecular oxygen at 25 eV, the equivalent neutral current density is about 5 mA/cm^2.

5. The Thruster

We now consider the quasi-neutral plasma nozzle as an ion thruster. In fact the thruster was one of the earliest envisioned applications of an ECR plasma [27,28]. Since the initial studies of the ECR thruster in the 60's, the solar power satellite (SPS) program has emerged [29]. Briefly, the SPS proposed putting large satellites in geosynchronous orbit, converting sunlight to microwaves, radiating it to the earth and converting it to electric power on the ground. While this program was studied by NASA and DoE, there were a large number of studies of magnetrons in space [30-33]. Even with the requirement for combining power from many different sources coherently and radiating it to the earth through large antennas, which would not be required for the thruster; the efficiency, lifetime and weight were all acceptable (except of course for the cost of getting it to geosynchronous orbit!). For instance Refs. [30-33] speak of magnetron efficiencies of 90%, lifetimes of 50-100 years, and weights of 0.7 kG/kW for the microwave generator and its power conditioner. Furthermore, studies of ECR plasmas have shown that in the configuration of Fig. 1a, right hand circularly polarized waves are absorbed with virtually 100% efficiency [10,11,13-16]. The configuration in Fig 1b also absorbs power efficiently [12]. Thus the results of studies from the SPS program, as well as those of ground based ECR plasmas provide an enormous knowledge base not available in the early days of ECR thrusters.

The most recent work on ECR thrusters appears to be that of Sercel [28]. He did theory and experiments on ECR argon plasmas in a thruster configuration, but at a lower pressure than the other ECR experiments we have cited. Using Fig. 5 with an assumed 30 cm length, and the pressures in his experiment, $2\text{-}4 \times 10^{-5}$ torr, we find the predicted electron temperature is about 25 eV as measured. The measured downstream ion streaming energy was about 70-100 eV, which is also reasonably consistent with the theory developed here.

For the thruster, we consider rare gases to be the preferred species so as to minimize corrosion by chemical reactions on the thruster wall and also to increase the ionization efficiency. The mass flow out the thruster is given by

$$\frac{dMass}{dt} = n_s M c_s A_s \qquad (29)$$

where all quantities are evaluated at the final sonic point x_s. This is the rate of fuel consumption assuming the ion flux exceeds the neutral flux.

Now let us consider the thrust by looking at the expelled plasma where the fuel has accelerated to a speed $\alpha_s c_s$. The plasma momentum flux times the area is the force on the rocket. The momentum flux at the exit point is $nMu^2 + nT_e$. Notice that not only the

escaping ions, but also the electron pressure contribute to the thrust. However this assumes that the electrons freely exit and are not inhibited by the magnetic field. We will discuss this further shortly. Assuming that nuA is constant in the acceleration region, we can relate the accelerating force to the quantities at the sonic point.

$$F = n_s A_s T_e \left(\alpha_s + \frac{1}{\alpha_s} \right) \tag{30}$$

Thus for the ECR thruster, the acceleration increases the force on the rocket. However it does so by increasing the ion force, but decreasing the electron pressure force. Another important parameter in thruster terminology is the specific impulse I_{sp} which is just the exhaust velocity $\alpha_s c_s$ divided by the gravitational acceleration. Desirable values for I_{sp} typically range from about 500 to 10^4 depending on the mission. If $\alpha=3$, a xenon plasma at 30 ev gives a specific impulse of about 1600 sec. At 30 ev, a helium plasma would give an I_{sp} of nearly 10^4.

An important consideration for a thruster is its efficiency. Martinez-Sanchez [4] defines efficiency as the power into the rocket $\alpha_s c_s F$, divided by twice the power to produce the plasma. The power to produce the plasma is given by Eq. (15). Then the efficiency η is

$$\eta = \frac{\left(\alpha^2 + 1 \right) n_s A_s}{\sum_a A_a n_a \left[\alpha_a^2 + 5 + \left(2E_i / T_e \right) \right]} \tag{31}$$

We have seen that a reasonable maximum estimate for α_s^2 is about ten, and of course α_w =1. Clearly there are two keys to increasing the efficiency, reducing E_i/T_e, and minimizing the power to the wall. If we consider a 30 ev xenon plasma with a thruster designed so that $A_w n_w = A_s n_s/2$, then the thruster is about 50% efficient.

We now briefly consider the expulsion of the accelerated plasma into space. There are both electric and magnetic considerations. We will start with the electric considerations. The space craft is assumed to be at the same potential as the space environment it travels through. The plasma, before it begins its acceleration is at a potential of approximately $\phi_{sh} + T/2e$ with respect to the left hand wall x_w. We assume for now that x_w is grounded to the spacecraft. The drop in plasma potential at the ejection point is approximately $0.5 M \alpha_s^2 T$. This is approximately equal to $\phi_{sh} + T/2e$. Let us consider the idealized case where the two are equal. In this case the plasma is ejected freely into space, and there is no additional acceleration or deceleration. If these potentials are not exactly equal, the left wall could be biased at some potential with respect to the spacecraft to make them equal.

If the final potential of the plasma upon ejection is not equal to the spacecraft potential, there would be some additional acceleration of the low density, time dependent plasma until such point as it finds itself to be at zero (i.e. the space craft) potential. There would also be electrostatic forces on the spacecraft which could further accelerate or decelerate it. Another possibility is to bias x_w above the spacecraft potential so as to increase the thrust. These are complicating aspects which we will not consider here.

Another important aspect of the expelled plasma is the plume divergence angle. For the surface confined plasma (Fig 1b) there is no magnetic field, so the plasma, freely exits from the exhaust. Also, since the ion temperature at the center of the plasma is small, the plume angle should be small. Since the electrons freely exit with the ions, there is no need for a separate electron to neutralize the ion flow. In that sense, the cusp configuration (Fig 1b) seems optimum for the thruster.

The axial field version (Fig 1a) has additional complications.. If the magnetic field configuration at the exit point is azimuthally symmetric, the ions must ultimately cross field lines to get out. Using the constancy of the canonical momentum in the θ direction, one can calculate the azimuthal ion velocity v_θ in the zero field region, and thereby estimate the plume angle. The ions can only escape if B_r at the exhaust point is below some maximum value proportional to the ion velocity.

Now let us consider the electron exhaust. If B_r is sufficiently small, the ions and electrons can set up an axial electrical field which can drag the electrons out with the ions. This is rather like the Hull cutoff in a magnetron. However as the electrons escape, they also pick up v_θ, and the $v_\theta B_r$ force is an additional retarding force on the spacecraft. If B_r is small enough that the ions can get out, but large enough that the electrons cannot, a neutralizing electron current from a source outside the field region may have to be injected. This is a standard practice for many thrusters [4], especially for a Hall thruster. Of course the magnetic field lines near the exit point do not have to be cylindrically symmetric. If the field lines all curve away in one direction, the centrifugal force on the streaming plasma will polarize it. This polarization generated electric field, enhanced by the high dielectric constant of the magnetized plasma will cause the plasma to ExB drift across the curving magnetic field. The result of this ExB drift is that that the plasma streams straight out across the field [34]. In this case, the plume angle will again be small, and there would be no need for a separate external electron source, since the electrons and ions cross the field together.

Thus regarding the plasma exhaust, the multiple cusp configuration, Fig. (1b), seems to have important advantages. For the axial field configuration, Fig. (1a), operation is still possible, especially if asymmetric exhaust of the plasma proves possible.

Exhausting the plasma through a symmetric field configuration appears to be possible, but difficult.

To summarize, the quasi-neutral plasma nozzle thruster has a number of potential advantages. These include high thrust, high specific impulse, high efficiency. Also there are no electrodes or fine screens anywhere, so its lifetime should be long. Finally the configuration has the possibility of eliminating the external electron source and operating with a quasi-neutral plasma everywhere so as to produce a very low plume angle.

References:

1. M. Lieberman and A. Lichtenberg, *Principles of Plasma Discharges and Material Processing*, p 161, Wiley and Sons, NY, 1994
2. ibid, p 158
3. T. Tsuchizawa et al, Jpn. J. Appl. Phys. 33, 2200, 1994
4. Y. Jin et al, Jpn. J. Appl. Phys. 34, Pt. 2 No. 4A L465, 1995
5. M. Martinez-Sanchez and J. Pollard, J. Propulsion and Power, 14, 688, 1998
6. K. Oswatitsch, *Gas Dynamics*, Chapter 2, Academic Press, NY, 1956
7. A.J. Hundhausen, *Coronal Expansion and Solar Wind*, Springer, NY, 1974
8. J. Ashkenazy, Phys. Lett., A 288, 369, 1977
9. K. Riemann, IEEE Trans. Plasma Sci. 23, 709, 1995
10. M. Lampe, G. Joyce, W. Manheimer, and S. Slinker, IEEE Trans. Plasma Sci. 26, 1592, 1998
11. C. Eddy et al, J. Vac. Sci. Technol. A 17, 38, 1999
12. J. Asmussen, J. Vac. Sci. Technol. A7, 883, 1989
13. M. Matsouka and K. Ono, J. Vac. Sci. Technol. A6, 25, 1988
14. T. Ono, M. Oda, C. Takahashi, and S. Matsou, J. Vac. Sci. Technol. B4, 69, 1986
15. Y. Okuno, Y. Ohtsu, and H. Fujita, IEEE Trans. Plasma Sci., 22, 253, 1994
16. N. Sadeghi, T. Nakano, D. Trevor, and R. Gottscho, J. Appl. Phys. 70, 2552, 1991
17. A. Fruchtman and N. Fisch, AIAA 98-3500, Joint Propulsion Conference, Cleveland, 1998
18. A. Fruchtman and N. Fisch, AIAA 99-2142, Joint Propulsion Conference, Los Angeles, 1999
19. R. Hake and A. Phelps, Phys. Rev, 158, 70, 1967
20. H. Ellis, R. Pai, and E. McDaniel, Atomic Data and Nuclear Tables, 17, 177, 1976
21. S. Brown, *Basic Data of Plasma Physics, 1966*, p 69, MIT Press, Cambridge, MA, 1967
22. ibid, p 57 and 73
23. ibid. p 141
24. O. Glembocki, private communication, Feb, 2000
25. J. Dutton, J. Phys. Chem. Reference Data, 4, 577, 1975
26. L. Christophorou, *Atomic and Molecular Radiation Physics*, p 36, J. Wiley and Sons, NY, 1971
27. D. Miller and G. Bethke, AIAA J. 4, 835, 1966
28. J. Sercel, Ph.D thesis, Cal. Tech. Dept of Aeronautics and Astronautics, 1993
29. P.E. Glaser, Science, 162, 857, 1968
30. W.C. Brown, IEEE Spectrum, June, 1979, p36
31. W.C. Brown, IEEE Trans. MTT, 29, 1391, 1981
32. W.C. Brown, Space Power, 6, 123, 1986
33. W.C. Brown, Space Power, 11, 27, 1992

34. G. Schmidt, Physics of High Temperature Plasmas, Chap 6.2, Academic Press, NY, 1966

Figure Captions:

Figure 1: The configuration of an ECR plasma with a) axial field, and b) multipole field. The dotted lines are magnetic field lines.

Figure 2: A plot of $F(T_e/\varepsilon_i)$ as a function of T_e/ε_i.

Figure 3: An upper limit for ion acceleration (E/T_e) as a function of plasma area divided by the area at the sonic point (A/A_o)

Figure 4: A plot of energy as a function of density for an accelerated plasma

Figure 5: A plot of electron temperature compared to ionization energy (T_e/ε_i) as a function of background pressure for an ECR plasma.

Figure 6: Experimental determination (circles) of ion acceleration in an ECR plasma as a function of pressure, and the theoretical estimate.

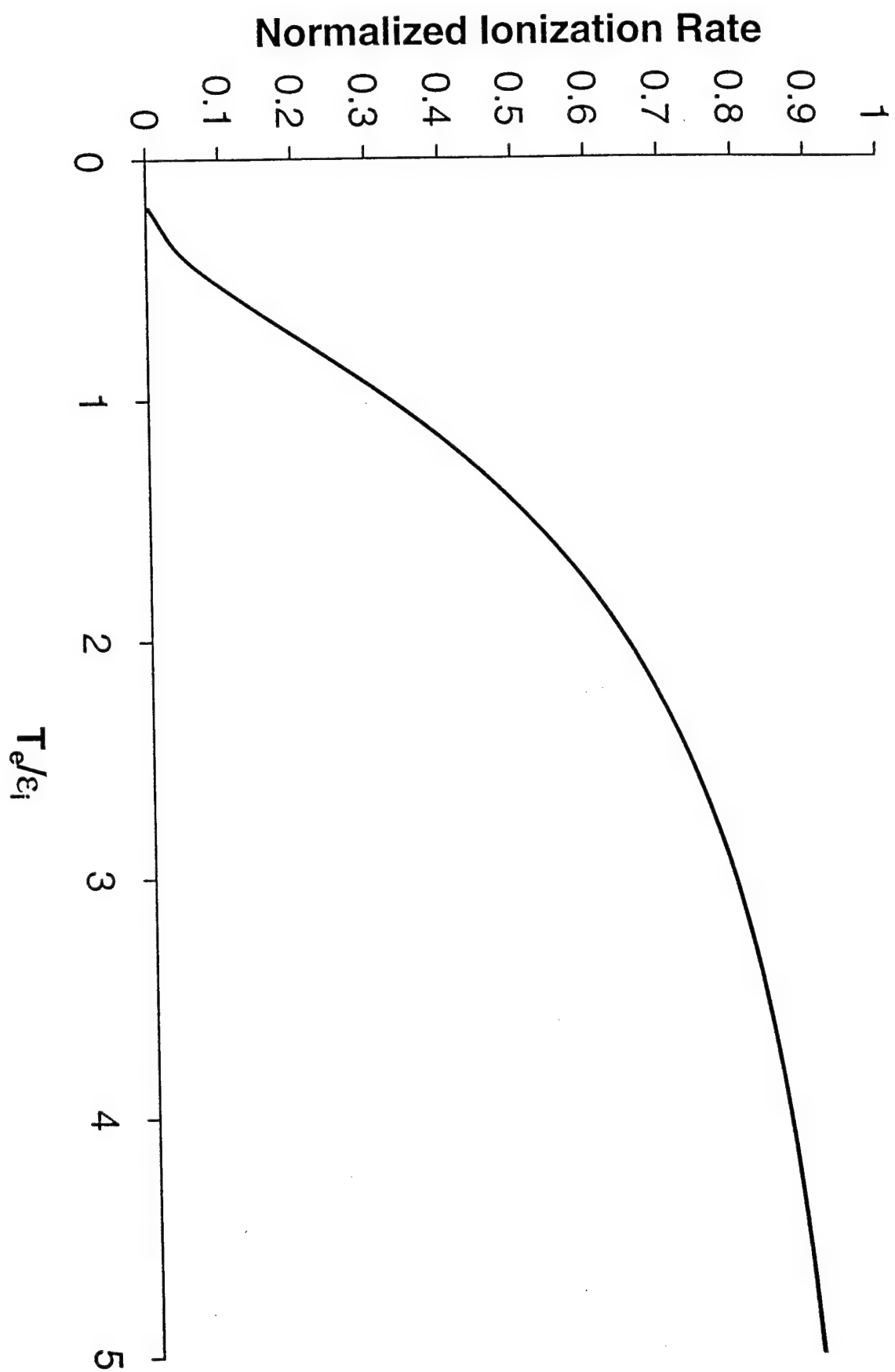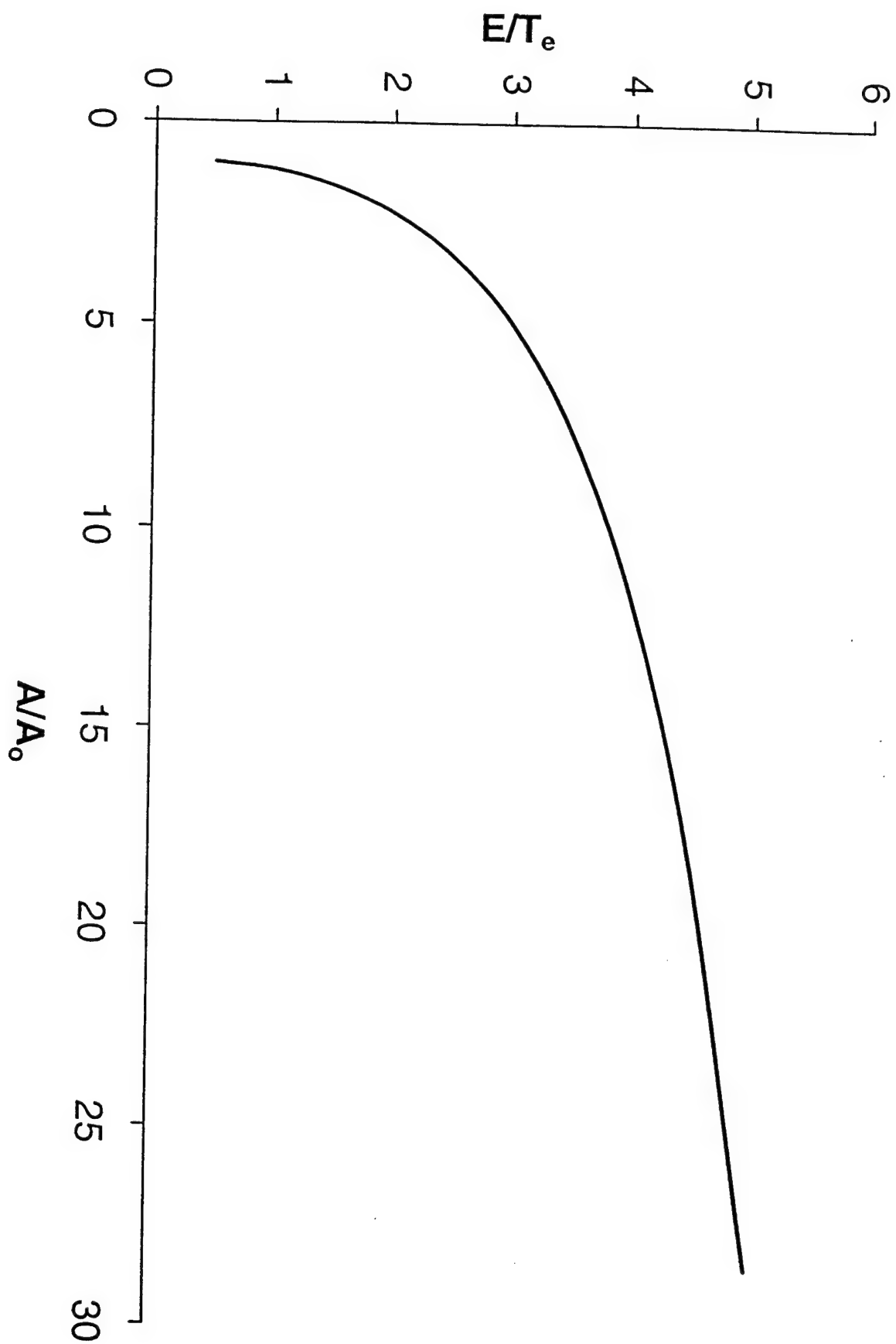Figure 7: The configuration of a neutral etcher. The dotted lines are magnetic field lines.
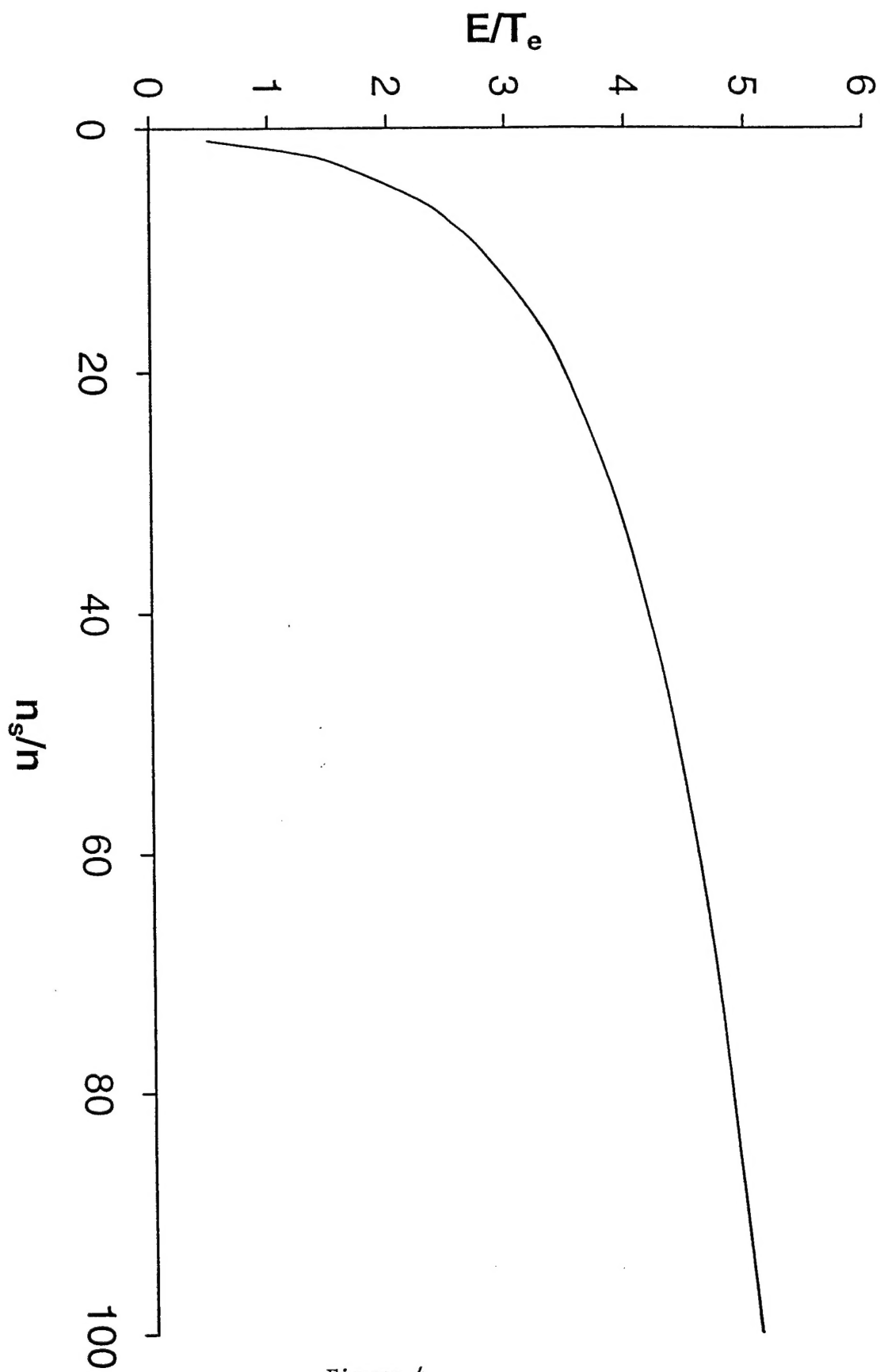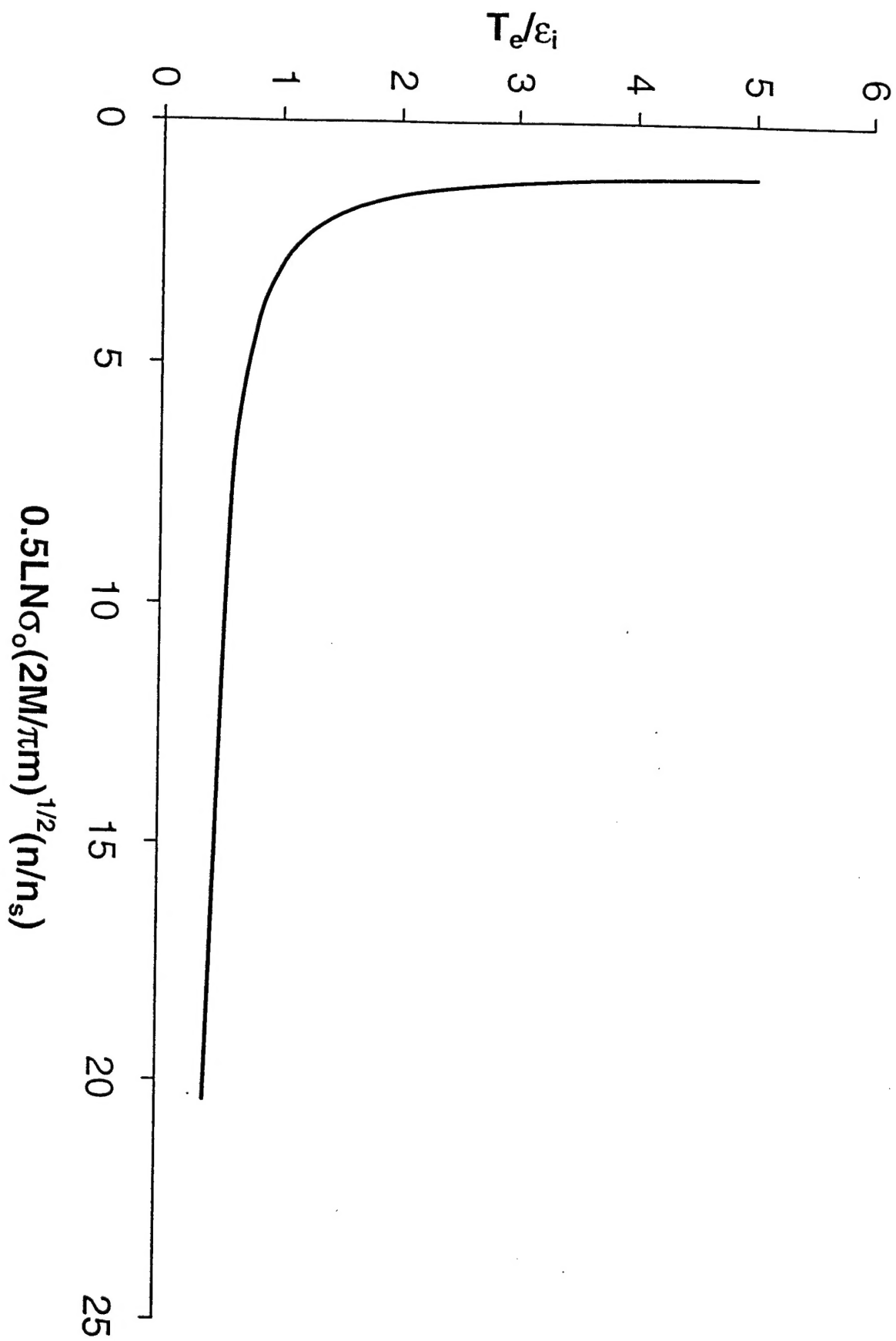
Figure 1

Figure 2

Figure 3.

Figure 4

Figure 5

Figure 6

PRODUCTION REGION

ACCELERATION REGION

CHARGE EXCHANGE AND FIELD DEFLECTION REGION

X_W

X_S

NEUTRAL STREAM (E ~ 40 eV)

FINAL FIELD DEFLECTOR

WORKPIECE

Figure   7